TURBULENCE IN GALAXY CLUSTER CORES: A KEY TO CLUSTER BIMODALITY?

Ian J. Parrish[1], Eliot Quataert, and Prateek Sharma[1]
Astronomy Department & Theoretical Astrophysics Center, 601 Campbell Hall, University of California Berkeley, CA 94720, USA;
iparrish@astro.berkeley.edu
Draft version March 30, 2010

ABSTRACT

We study the effects of externally imposed turbulence on the thermal properties of galaxy cluster cores, using three-dimensional numerical simulations including magnetic fields, anisotropic thermal conduction, and radiative cooling. The imposed "stirring" crudely approximates the effects of galactic wakes, waves generated by galaxies moving through the intracluster medium (ICM), and/or turbulence produced by a central active galactic nucleus. The simulated clusters exhibit a strong bimodality. Modest levels of turbulence, $\sim 100\,\mathrm{km\,s^{-1}} \sim 10\%$ of the sound speed, suppress the heat-flux-driven buoyancy instability (HBI), resulting in an isotropically tangled magnetic field and a quasi-stable, high entropy, thermal equilibrium with no cooling catastrophe. Thermal conduction dominates the heating of the cluster core, but turbulent mixing is critical because it suppresses the HBI and (to a lesser extent) the thermal instability. Lower levels of turbulent mixing ($\lesssim 100\,\mathrm{km\,s^{-1}}$) are insufficient to suppress the HBI, rapidly leading to a thermal runaway and a cool-core cluster. Remarkably, then, small fluctuations in the level of turbulence in galaxy cluster cores can initiate transitions between cool-core (low entropy) and non cool-core (high entropy) states.

Subject headings: convection—galaxies: clusters: general—instabilities—MHD—plasmas

1. INTRODUCTION

The cooling time in the intracluster medium (ICM) of galaxy clusters is often $\lesssim 0.1$–1 Gyr near the center of the cluster (Sarazin 1986). X-ray spectroscopy shows, however, that the majority of the plasma is not in fact cooling to temperatures well below the mean cluster temperature (e.g., Peterson & Fabian 2006). Understanding the processes responsible for heating and stabilizing cluster plasmas is a central problem in galaxy formation. Some of the most promising energy sources include a central active galactic nucleus (AGN) (e.g., Binney & Tabor 1995), thermal conduction from large radii (e.g., Narayan & Medvedev 2001), or dynamical friction and/or turbulence generated by the motion of substructure through the cluster (e.g., Kim et al. 2005). In this *Letter* we show that although neither of the latter two mechanisms works on its own, together they have novel implications for the thermodynamics of the ICM.

The central parts of clusters are unstable to a convective instability driven by the anisotropic flow of heat along magnetic field lines (the HBI; Quataert 2008). Simulations of the HBI show that it saturates by preferentially reorienting the magnetic field lines to be perpendicular to the temperature gradient, thus reducing the effective radial conductivity of the plasma (Parrish & Quataert 2008; Bogdanović et al. 2009; Parrish et al. 2009, hereafter PQS). This exacerbates the cooling catastrophe by making it difficult to tap into the thermal bath at large radii, particularly for clusters with low central entropies and short central cooling times.

Previous simulations of the HBI in clusters have focused on idealized problems in which the HBI was the primary source of turbulence (Sharma et al. 2009a also studied the role of convection driven by cosmic-rays).

There are, however, many additional sources of turbulence in clusters, including major mergers, the motion of galaxies through the ICM (galaxy wakes), and AGN jets and bubbles. Cosmological hydrodynamic simulations of cluster formation find that turbulence can contribute ~ 1–10% of the total pressure even in relaxed clusters, with the turbulent pressure declining at small radii towards the cluster core (Lau et al. 2009).

In this *Letter*, we consider a simple model for the interplay between turbulence, anisotropic thermal conduction, and radiative cooling in galaxy cluster cores: we externally "stir" the ICM in our previous global cluster core simulations (e.g., PQS) in order to mimic the effects of the various sources of turbulence noted above. The limitations of this approach are discussed in §4.

Near the completion of this work, Ruszkowski & Oh (2009) presented results similar to those found here using independent numerical techniques and cluster models.

2. METHODS

We solve the equations of MHD using the `Athena` MHD code (Gardiner & Stone 2008; Stone et al. 2008), with the addition of anisotropic thermal conduction (Parrish & Stone 2005; Sharma & Hammett 2007) and optically thin cooling (see eqs [8]–[12] of PQS). In particular, the conductive heat flux is given by $\boldsymbol{Q} = -\kappa_{\mathrm{Sp}}\hat{\boldsymbol{b}}\hat{\boldsymbol{b}}\cdot\boldsymbol{\nabla}T$, where κ_{Sp} is the Spitzer thermal conductivity and $\hat{\boldsymbol{b}}$ is a unit vector along the magnetic field. We use the Tozzi & Norman (2001) cooling curve and a temperature floor of $T = 0.05\,\mathrm{keV}$, below which UV lines become important.

Our initial condition is a cluster inspired to resemble that of Abell 2199 as observed in Johnstone et al. (2002). We use a static NFW gravitational potential with a scale radius of $r_s = 390\,\mathrm{kpc}$ and a mass of $M_0 = 3.8\times10^{14}M_\odot$. The simulations are carried out on a Cartesian grid in a computational domain that extends from the center of

---

[1] Chandra/Einstein Fellow

the cluster out to 240 kpc. The simulations are (128^3), corresponding to a resolution of 3.4 kpc. Resolution studies indicate that our conclusions are not sensitive to resolution. We begin with an ICM that is in both hydrostatic and thermal equilibrium, with conduction balancing cooling; simulations without initial thermal equilibrium showed large thermal transients. The resulting model cluster has a central temperature and electron density of $\simeq 1.3$ keV and $\simeq 0.04\,\mathrm{cm}^{-3}$, respectively, and a temperature and density of 5 keV and $2 \times 10^{-3}\,\mathrm{cm}^{-3}$ near 200 kpc. The magnetic field is initially tangled, with $\langle |B| \rangle = 10^{-9}$ G and a Kolmogorov power spectrum. Further details of our initial conditions can be found in sections 3–4 of PQS.

Our model clusters do not include the turbulence that would realistically be generated by the hierarchical growth of structure or a central AGN. To crudely account for this, we continuously add an additional random velocity to our cluster models. We drive the velocity fields in Fourier space using the methods described in Lemaster & Stone (2009). For a given driving length scale L, we drive velocities with a flat spectrum in Fourier space on scales corresponding to $L \pm 10$ kpc. We clean the spectrum so that the motions are incompressible and Fourier transform to real space normalizing to the desired level of turbulence. This results in rms velocities, δv, that are uniform throughout the cluster. Note that our stirring is statistically steady in both time and space. This is not necessarily a good approximation in clusters—we return to this point in §4.

Our fiducial turbulence parameters are $\delta v \sim 50$–$100\,\mathrm{km\,s^{-1}}$ and $L \sim 40$–100 kpc. This corresponds to turbulence that contributes a few % of the total pressure in the cluster core. The strength of the turbulence produced by galaxies moving through the ICM can be estimated by calculating the total power dissipated by dynamical friction (e.g., eqn. [4] of Kim et al. 2005). Assuming that this energy is ultimately dissipated via a turbulent cascade, we find

$$\delta v \sim c_s \left(\frac{GM_g}{c_s^2 R} \right)^{2/3} \left(\frac{6N_g L}{R} \right)^{1/3}, \qquad (1)$$

where M_g is the mass of a typical galaxy, N_g is the number of galaxies, R is the size of the region of interest, and c_s is the sound speed of the ICM. For five $10^{11} M_\odot$ galaxies within 200 kpc and a turbulent scale of $L \sim 40$ kpc, equation (1) implies $\delta v \sim 0.08 c_s$, consistent with our fiducial numbers quoted above. In reality, the generation of turbulence by galaxies moving through the ICM will be more subtle, with some of the energy going into sound waves and gravity waves, and some being confined to galactic wakes correlated with the orbits of galaxies.

3. RESULTS

To illustrate the effect that turbulence can have on the thermal evolution of galaxy clusters, Figure 1 shows the late-time azimuthally averaged temperature profile for simulations of the same cluster with different rms turbulent velocities, δv, and thus also different turbulent heating rates $\dot{e}_{\mathrm{turb}} \simeq \rho (\delta v)^3 / L$. For low turbulent velocities, the evolution is similar to that found previously by PQS: the HBI reorients the magnetic field to be perpendicular to the radial temperature gradient, shutting off
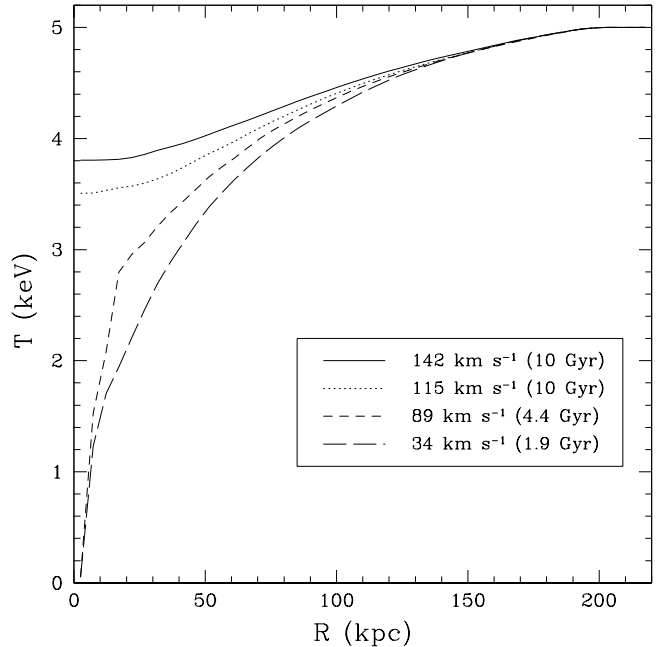

Fig. 1.— Azimuthally-averaged temperature profiles for identical cluster cores with different imposed rms turbulent velocities (see legend); the driving scale is fixed at $L = 40$ kpc. A strong bimodality in cluster properties results. Stronger driving ($\delta v \gtrsim 100\,\mathrm{km\,s^{-1}}$) leads to a roughly stable thermal profile (shown at 10 Gyr). Somewhat weaker driving leads to a cooling catastrophe (shown at the onset of the cooling catastrophe). Eqn. 2 quantifies the level of turbulent mixing required to suppress the HBI and transition from the low temperature, low entropy state, to the high temperature, high entropy state.

heat conduction from large radii and thus precipitating a cooling catastrophe in the cluster core. The cluster core reaches the temperature floor at $\simeq 1.9$ Gyr in our lowest δv simulation. For larger $\delta v \gtrsim 100\,\mathrm{km\,s^{-1}} \sim 0.1\,c_s$, however, the dynamics changes completely. The magnetic field remains relatively isotropic at all times, indicating that the HBI is no longer acting effectively. Moreover, the cluster reaches a stable equilibrium, with the temperature profiles shown in Figure 1 remaining roughly the same for the last $\simeq 5$–7 Gyr of the simulation. It is important to stress that even for $\delta v \sim 100\,\mathrm{km\,s^{-1}}$, the heating rate due to the turbulence is negligible compared to the cooling rate and thus the turbulence is energetically unimportant for the thermal properties of the cluster (§4). Note also that the central temperature increases slightly as the turbulent energy increases in Figure 1; we attribute this to the increased advective (turbulent) heat transport associated with the higher turbulent velocities.

To quantify in more detail the effect of turbulence on the evolution of cluster plasmas, Figure 2 shows the temperature and magnetic field direction as a function of radius at several different times for two simulations (labeled A and B) whose properties are summarized in Table 1 (case C in Table 1 is discussed below). The simulations are again of identical clusters and both include turbulence with $\delta v \sim 100\,\mathrm{km\,s^{-1}}$, near the threshold for the transition from stability to instability in Figure 1. The simulations differ in that case A has a turbulent correlation length of $L = 40$ kpc, while B has $L = 100$ kpc; as a result, simulation A has a heating rate $\dot{e}_{\mathrm{turb}}$ that is 2.5

TABLE 1
PROPERTIES OF THE FIDUCIAL SIMULATIONS[a]

Run	$\langle \dot{e}_{\rm turb} \rangle$ (erg cm^{-3} s^{-1})	L (kpc)	δv (km s^{-1})	$t_{\rm cool}$ (Myr)	$t_{\rm HBI}$ (Myr)	$t_{\rm eddy}(L)$ (Myr)	$t_{\rm eddy}(\lambda_F)$ (Myr)	$K_0^{\rm final}$ (keV cm^2)
A	7.5×10^{-30}	40	115	400	100	400	360	53
B	3.0×10^{-30}	100	112	400	100	1000	490	0.06
C	3.0×10^{-29}	100	250	400	100	390	195	110

[a] Timescales are estimated at the initial time, while the turbulent velocity and central entropy are measured in the saturated state for runs A & C, and just before the cooling catastrophe for run B. The Field length is estimated near the cluster center, while $\dot{e}_{\rm turb}$ is volume averaged.
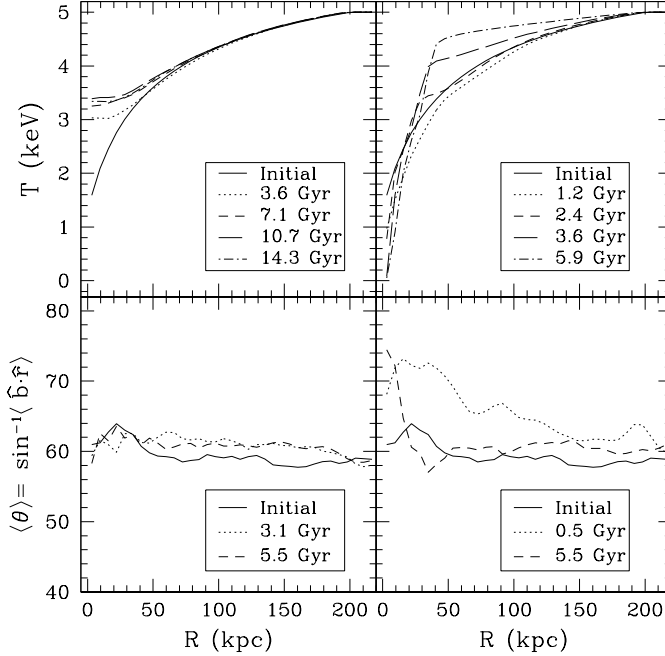

FIG. 2.— Azimuthally-averaged profiles for simulations with imposed turbulence having the same $\delta v \simeq 112\,{\rm km\,s^{-1}}$, but different correlation lengths. Run A (*left*) has $L = 40$ kpc, while run B (*right*) has $L = 100$ kpc (see Table 1) *Top:* Temperature profiles. *Bottom:* Magnetic field angle relative to the radial: 60° corresponds to an isotropically tangled magnetic field and an effective radial conductivity $\sim 1/3$ Spitzer. Run A (*left*), with the shorter turbulent mixing time, reaches a stable state averting the cooling catastrophe. In Run B (*right*), the HBI persists, shutting off conduction and initiating a cooling catastrophe.

times higher and an eddy turnover time on scale L that is 2.5 times shorter.

Despite their similarities, the top panels of Figure 2 show dramatic differences in the evolution of the clusters' radial temperature profile. Simulation B proceeds with little regard for the turbulent driving. The HBI reorients the magnetic field, reducing the effective radial thermal conductivity, and hastening the onset of the cooling catastrophe at $\simeq 2.2$ Gyr. On the other hand, simulation A is dramatically affected by the turbulent driving, just like the high δv simulations in Figure 1. In this case the turbulence effectively shuts off the HBI, with the mean angle of the magnetic field from radial fluctuating about the isotropic value of $\langle \theta_B \rangle \sim 60°$.

In addition to suppressing the effects of the HBI, the presence of "sufficient" turbulence also appears to modify the thermal stability of the cluster. Case A in Figure 2 shows that the cluster reaches a statistically stable thermal equilibrium that survives for longer than the age

of the universe. The stability of the new equilibrium is illustrated by the fact that the cluster's central temperature undergoes slight oscillations about a new equilibrium value.

4. INTERPRETATION AND DISCUSSION

It is important to stress that for all of the simulations presented here, the heating produced by the turbulence is energetically subdominant (this is also consistent with the modest dynamical friction heating in clusters inferred using observed galaxies; e.g., Kim et al. 2005). For simulation A in Figure 2, e.g., the turbulent heating rate per unit volume at the center of the computational domain is $\lesssim 2\%$ of the central cooling rate throughout the evolution of the cluster. As a result, the physics important for the results in Figures 1 & 2 includes anisotropic thermal conduction, the HBI, the thermal instability of cluster plasmas (Field 1965), and the mixing produced by the turbulence—but not the heating by such turbulence.

In general the global thermal instability of cluster plasmas in the presence of thermal conduction manifests itself as either catastrophic cooling in the core of the cluster, or overheating and the approach to an isothermal temperature profile (e.g., Conroy & Ostriker 2008; PQS). Which of these is realized in a given problem depends in part on the initial state of the system and boundary conditions. In cluster simulations without externally imposed turbulence, the HBI biases the nonlinear evolution of the thermal instability towards the cooling catastrophe by thermally decoupling the core from larger radii.

Our simulations show that if turbulence is sufficiently strong in cluster cores it can effectively shut off the HBI, leaving the magnetic field tangled and relatively isotropic, and the cluster with a quasi-steady, not-quite-isothermal temperature profile (Figs. 1 & 2). Quantitatively, turbulence with $\delta v \gtrsim 100\,{\rm km\,s^{-1}}$ or a Mach number $\gtrsim 0.1$ appears sufficient. More precisely, we believe that the critical criterion is (Sharma et al. 2009b)

$$t_{\rm eddy}(L) \simeq \frac{L}{\delta v} \lesssim \xi\,t_{\rm HBI} \simeq \xi \left(g \frac{d\ln T}{dr} \right)^{-1/2} \qquad (2)$$

where $t_{\rm eddy}(L)$ is the timescale for the turbulence to mix the plasma at the outer scale, $t_{\rm HBI}$ is the HBI growth time, g is the local gravitational acceleration in the cluster, and ξ is a dimensionless constant that must be determined from the simulations. Note that because the mixing timescale is smaller on smaller scales in a Kolmogorov cascade, the timescale inequality in equation (2) is the most difficult to satisfy at the outer scale.

Figure 2 demonstrates explicitly that a given value of δv is *not* in fact sufficient to suppress the HBI and halt the cooling catastrophe. Rather, this only occurs in run

A, which has a smaller correlation length L and shorter mixing time than run B (Table 1). Table 1 shows the properties of a third simulation not in Figure 2, in which the correlation length is the same as in run B ($L = 100$ kpc), but the turbulent velocity is larger. This combination again satisfies equation (2) and so the evolution is qualitatively similar to run A. Because the HBI growth time is ~ 100 Myr at ~ 50 kpc in these models, our numerical results correspond to $\xi \simeq 5$–8 in eq. (2).

In addition to its effects on the HBI, turbulent mixing can also significantly modify the thermal stability of cluster plasmas. Independent of turbulent mixing, thermal instability is stabilized on small scales (along the magnetic field) by thermal conduction. The critical length-scale below which conduction suppresses thermal instability (the Field length) is given by

$$\lambda_F \equiv \left[\frac{4\pi^2 T \kappa(T)}{n_e n_p \Lambda(T)} \right]^{1/2} \approx 53\,\mathrm{kpc} \left[\frac{K}{15\,\mathrm{keV\,cm^2}} \right]^{3/2}, \quad (3)$$

where $\Lambda(T)$ is the cooling function and we have used the full Spitzer conductivity in the final expression; in the second equality we have also assumed for simplicity that the cooling is pure bremsstrahlung so that λ_F can be expressed solely in terms of the entropy $K = T n_e^{-2/3}$ (Donahue et al. 2005).

Absent turbulence, fluctuations with length-scales $\gtrsim \lambda_F$ are unstable on a cooling time t_{cool}. If, however, turbulent mixing is sufficiently rapid, i.e., if

$$t_{\mathrm{eddy}}(\lambda_F) \lesssim t_{\mathrm{cool}}, \quad (4)$$

then turbulent mixing will suppress the thermal instability on the scale of the Field length, although larger length-scale fluctuations may remain unstable; local simulations of thermal instability in the presence of background turbulence confirm this intuition (these will be presented elsewhere). Table 1 shows that for both runs A and B in Figure 2, $t_{\mathrm{eddy}}(\lambda_F) \sim t_{\mathrm{cool}}$; that is, the modest turbulence levels considered here are capable of significantly changing the dynamics of the thermal instability in cluster plasmas. One extreme limit of this is the possibility that turbulent mixing of hot gas from large radii with cooler gas from small radii can help prevent the cooling catastrophe (ZuHone et al. 2009). In our stable simulations, however, (e.g., Case A) this is not realized: thermal conduction (not turbulent mixing) provides the dominant source of heating at small radii. The key role of the turbulent mixing is that it suppresses the HBI, isotropizes the magnetic field, and helps suppress the thermal instability by mixing the plasma before it can cool. This dynamics is qualitatively analogous to the critical role that turbulence plays in mixing and disrupting laminar conductive flames in the combustion and Type Ia supernova contexts (e.g., Peters 2000; Woosley 2007, respectively).

In our simulations, the interaction between turbulence, the HBI, and cooling leads to a strong bimodality in the cluster properties (e.g., temperature profiles). Figure 1 shows that runs with moderately strong turbulence (satisfying eqn. [2]) reach a quasi-stable thermal equilibrium averting the cooling catastrophe. By contrast, runs with slightly weaker turbulence—δv smaller by just $\sim 25\%$—progress to a cooling catastrophe on a timescale as short as a few central cooling times (much like the pure HBI simulations of PQS and Bogdanović et al. 2009).

It is tempting to relate this behavior to the observed variety in galaxy cluster properties. Observationally, clusters show a bimodality in their central gas entropies and cooling times, with lower entropy clusters preferentially having more star formation and Hα emission, and more powerful AGN (Voit et al. 2008; Cavagnolo et al. 2009); the transition occurs at $\simeq 30$ keV cm^2. This bimodality is closely related to the well-known fact that clusters come in both cool core and non cool core varieties (see Hudson et al. 2009).

The observed bimodality in cluster properties is not well understood. Burns et al. (2008) argued that early major mergers could prevent the formation of cool core clusters. Alternatively, Guo et al. (2008) showed using both 1D time dependent models and a global stability analysis that the combination of AGN feedback and scalar conduction can produce a bimodal population of stable cluster models; in their models AGN heating largely balances cooling in lower entropy clusters while conduction is more important in higher entropy clusters. They further suggested that AGN feedback could transition clusters from low to high entropy (Guo & Oh 2009).

Our simulations demonstrate that a low entropy cool-core cluster can transition to a significantly higher entropy state: run A initially has a central entropy of $K_0 \approx 11$ keV cm^2 while its final central entropy is $K_0 \approx 57$ keV cm^2. Run C is the same as run B but with a higher δv; its final central entropy is $K_0 \sim 110$ keV cm^2. This increase in central entropy is a consequence of runaway conductive heating at the roughly fixed pressure required for hydrostatic equilibrium. Physically, such a transition could occur if a cluster initially had little turbulence and inefficient conduction (because of the HBI), but was stabilized by a central AGN. The sudden onset of turbulence satisfying equation (2)—produced by an infalling galaxy or the AGN—would isotropize the magnetic field and suppress the HBI. The cluster would then evolve as in Figure 2 (*left panel*; case A) to a higher entropy state. If the turbulence in the cluster core later died away, the HBI would rapidly rearrange the magnetic field (Fig. 1), leading to cooling of the core after ~ 1 Gyr and (by assumption) increased AGN activity that would again stabilize the cluster in a cool-core state. This demonstrates that modest levels of turbulence in cluster cores ($\delta v \sim 100$ km s^{-1}; eqn. [2]) can have a dramatic affect on their thermal evolution. Note also that the energy required to generate turbulence capable of suppressing the HBI and thermal instability is far less than that required to directly increase the entropy of the cluster (as in Guo & Oh 2009).

Our calculations are based on an overly-simplified treatment of turbulence in galaxy cluster plasmas. Real turbulence in clusters is likely to be more intermittent in space and time than our model (§2), depending on, e.g., the distance to an AGN jet or a galactic wake. Waves generated by AGN jets and bubbles and/or galaxies moving through the ICM may produce reasonably volume-filling turbulence in cluster cores, but this needs to be studied in detail. Provided that the turbulence is replenished on $t_{\mathrm{cool}} \sim 0.1$–1 Gyr, our results will be relatively unchanged. Otherwise, the HBI and thermal instability will proceed unchecked. This temporal and spatial intermittency of turbulence in cluster cores may ultimately prove to be a positive feature, not a "bug,"

of our model: as described above, modest changes in the level of turbulence in clusters can produce rapid and dramatic changes in the thermal structure and stability of the cluster, to the point of initiating transitions from low to high entropy states (and vice-versa). Overall, the subtle interaction between turbulence, the HBI, and cooling in galaxy cluster cores has a surprisingly large impact on the thermal properties of the ICM. The critical role of the turbulence is not the small amount of turbulent energy dissipated (which is $\ll$ the cooling luminosity); rather, it is the fact that turbulent mixing can suppress both the HBI and the thermal instability in cluster cores (see eqs. [2] and [4], respectively).

REFERENCES

Binney, J., & Tabor, G. 1995, MNRAS, 276, 663
Bogdanović, T., Reynolds, C. S., Balbus, S. A., & Parrish, I. J. 2009, ApJ, 704, 211
Burns, J. O., Hallman, E. J., Gantner, B., Motl, P. M., & Norman, M. L. 2008, ApJ, 675, 1125
Cavagnolo, K. W., Donahue, M., Voit, G. M., & Sun, M. 2009, ArXiv:0902.1802
Conroy, C., & Ostriker, J. P. 2008, ApJ, 681, 151
Donahue, M., Voit, G. M., O'Dea, C. P., Baum, S. A., & Sparks, W. B. 2005, ApJ, 630, L13
Field, G. B. 1965, ApJ, 142, 531
Gardiner, T. A., & Stone, J. M. 2008, Journal of Computational Physics, 227, 4123
Guo, F., & Oh, S. P. 2009, MNRAS, 1478
Guo, F., Oh, S. P., & Ruszkowski, M. 2008, ApJ, 688, 859
Hudson, D. S., Mittal, R., Reiprich, T. H., Nulsen, P. E. J., Andernach, H., & Sarazin, C. L. 2009, ArXiv e-prints
Johnstone, R. M., Allen, S. W., Fabian, A. C., & Sanders, J. S. 2002, MNRAS, 336, 299
Kim, W., El-Zant, A. A., & Kamionkowski, M. 2005, ApJ, 632, 157
Lau, E. T., Kravtsov, A. V., & Nagai, D. 2009, ApJ, 705, 1129
Lemaster, M. N., & Stone, J. M. 2009, ApJ, 691, 1092
Narayan, R., & Medvedev, M. V. 2001, ApJ, 562, L129

Parrish, I. J., & Quataert, E. 2008, ApJ, 677, L9
Parrish, I. J., Quataert, E., & Sharma, P. 2009, ApJ, 703, 96
Parrish, I. J., & Stone, J. M. 2005, ApJ, 633, 334
Peters, N. 2000, Turbulent Combustion, ed. N. Peters
Peterson, J. R., & Fabian, A. C. 2006, Phys. Rep., 427, 1
Quataert, E. 2008, ApJ, 673, 758
Ruszkowski, M., & Oh, S. P. 2009, ArXiv e-prints
Sarazin, C. L. 1986, Reviews of Modern Physics, 58, 1
Sharma, P., Chandran, B. D. G., Quataert, E., & Parrish, I. J. 2009a, ArXiv:0901.4786
—. 2009b, ArXiv e-prints
Sharma, P., & Hammett, G. W. 2007, Journal of Computational Physics, 227, 123
Stone, J. M., Gardiner, T. A., Teuben, P., Hawley, J. F., & Simon, J. B. 2008, ApJS, 178, 137
Tozzi, P., & Norman, C. 2001, ApJ, 546, 63
Voit, G. M., Cavagnolo, K. W., Donahue, M., Rafferty, D. A., McNamara, B. R., & Nulsen, P. E. J. 2008, ApJ, 681, L5
Woosley, S. E. 2007, ApJ, 668, 1109
ZuHone, J. A., Markevitch, M., & Johnson, R. E. 2009, ArXiv e-prints